The 2010 IEEE/RSJ International Conference on
Intelligent Robots and Systems
October 18-22, 2010, Taipei, Taiwan

A Full-Body Motion Control Method for a Humanoid Robot based on On-Line Estimation of the Operational Force of an Object with an Unknown Weight

Shunichi Nozawa, Ryohei Ueda, Youhei Kakiuchi, Kei Okada and Masayuki Inaba

Abstract— **In this paper we propose a new method to manipulate heavy objects for a humanoid robot. In this method the manipulation strategy is determined based on on-line estimation of the operational force. We integrate these functions with a real-time controller that controls the external force and maintains full-body balance.**

The feature point of our work is that since a full-body control system includes switching of the manipulation strategy based on the operational force estimated on-line the system enables a humanoid robot to manipulate heavy objects as well as light objects. The effectiveness of our whole system is confirmed in our experiments, in which a humanoid robot manipulates up to 12[kg] while estimating the object's weight.

I. INTRODUCTION

Handling heavy objects is one of the most important tasks for robots because it is applicable not only to the various tasks of the daily life of the humans but also nursing care tasks. Because object manipulation is a significant topic in robotics, a lot of work in this area has enabled robots to handle lightweight objects by integrating visual feedback and complicated task planning. Several works have challenged a humanoid robot to manipulate heavy objects[1].

There are many problems related to the manipulation of of heavy objects by humanoid robots. (a) There are many strategies for manipulation such as single-armed manipulation, dual-armed manipulation or fullbody contact manipulation. It is difficult to determine a suitable strategy based on the operational force dependent on the mass property and the friction of objects. (b) In many cases it is difficult to accurately describe these parameters. In manipulation an object with an unknown weight, it is impossible to determine the strategy without trial and error. (c) Furthermore, in the case of manipulation by a humanoid robot, the constraints for reactive force and full-body humanoid robot balancing are both important.

In this paper to deal with the above problems we propose a new control system, which is a controller used for controlling the external force and full-body balancing (for (c)) including the function to determine the manipulation strategy based on on-line estimation of the operational force (for (a) and (b)). Related works challenged a humanoid robot to manipulate heavy objects [2], [3]. The advantage of our work is that since a full-body control system includes switching of the manipulation strategy based on the operational force estimated on-line, the system enables a humanoid to manipulate heavy objects as well as light objects. Our method is not specific to handling heavy objects[4].

S. Nozawa, R. Ueda, Y. Kakiuchi, K. Okada and M. Inaba are with Department of Mechano-Infomatics, The University of Tokyo, 7-3-1 Hongo, Bunkyo-ku, Tokyo 113-8656, Japan nozawa@jsk.t.u-tokyo.ac.jp

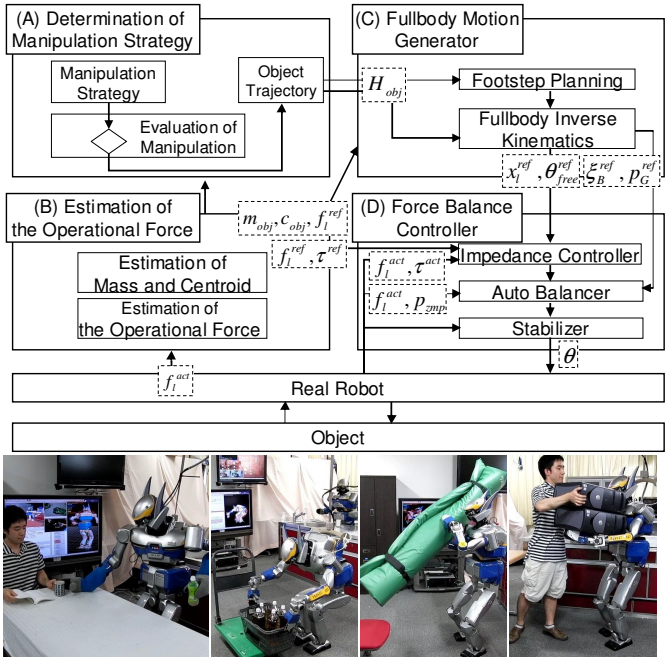

Fig. 1. The Whole Configuration of our System
Top figure : The system configuration for full-body manipulation
The lower snapshots : The examples in which a humanoid robot manipulates lightweight and heavyweight objects

The effectiveness of our control system is confirmed in two experiments. In one experiment in which a humanoid robot manipulates a 6 to 10[kg] object, the validity of the force and balancing controller with estimation of the operational force is shown. In another experiment in which a humanoid robot carries a 12[kg] object, the usefulness of manipulation strategy switching is shown.

II. FULL-BODY MANIPULATION OF A HEAVY OBJECT BY A HUMANOID ROBOT

In this section, we introduce a method to manipulate an object with an unknown weight for a humanoid robot. When a humanoid robot manipulates a heavy object, it is necessary to control the reaction force in order to avoid overload on each joint and to maintain full-body balance in order to

prevent the humanoid robot from falling down. In case of handling an object with an unknown weight, the system also should include on-line estimation of the operational force. If a humanoid robot cannot carry the object, the humanoid robot has to try different manipulation strategy. For example, if the humanoid robot cannot pick up an object using a single arm, the humanoid robot has to try using both arms.

We propose a full-body control system to satisfy the above mentioned constraints. Fig.1 shows the system configuration. We assume that the information about the shape of the object and where to grasp is known and the weight and the friction coefficient are unknown. First, the system selects one strategy from several strategies for manipulation and decides the trajectory of the object H_{obj} (module (A) in Fig.1). Second, a full-body motion sequence of the humanoid robot is generated based on the trajectory (module (C) in Fig.1). Third, the humanoid robot executes the sequence while controlling the reaction force and maintaining full-body balance (module (D) in Fig.1). While manipulating the object, the humanoid robot interacts with it. The system estimates the operational force based on the reaction force (module (B) in Fig.1) and feeds back the estimated state of the object to (A), (B) and (C). According to the feedback information about the object such as the mass m_{obj}, the centroid c_{obj} and the operational force f_l^{ref}, (A) switches the strategy for manipulation, (C) generates the motion sequence again and (D) controls the reaction force using the operational force as the command force. The symbols not mentioned above will be explained following sections.

In comparison to related works dealing with the manipulation of heavy objects [2], [3], [4], advantage of our full-body control system is that it has the ability to determine a manipulation strategy based on the operational force. Since the control system enables a humanoid robot to manipulate heavy objects as well as light objects, our system utilizes the several works discussed in manipulation of light weight objects [5].

The control method proposed in this paper is applicable to the position-controlled robot with several force sensors: our control system finally outputs a full-body posture sequence. Note that several control methods used to control the external force and maintain full-body balance are developed for a humanoid robot by Sentis et al. [6], Hyon et al. [7] and so on. Evard et al. [8] also proposed a force and balancing control algorithm for a position-controlled humanoid robot. The feature point of our system is that the force and balancing controller (module (D)) implemented in a high frequency process are separated from the motion generation (module (C)) based on multitasks such as using inverse kinematics to satisfy the trajectory of the object, footprint constraints and so on. Therefore we can add several modules to the high frequency processes except the force and balancing controller. We will explain this in detail in IV.

In the following sections we describe in detail the configuration of each modules. Modules (A) and (B) are introduced in III and module (D) is introduced in IV. We implement the proposed method on HRP2-JSK[9]. The integrated experiments are shown in V.

III. DETERMINING OF MANIPULATION STRATEGY AND ESTIMATING OF THE OPERATIONAL FORCE

In general how to manipulate an object is decided according to the shape, the mass properties of the object and other heuristics . Our control system is applicable to an object whose weight before manipulation is unknown to the robot. In this case the mass properties of the object are updated and the robot must replan how to manipulate it. In this section we describe manipulation switching and estimation of the operational force.

A. Determination of Manipulation Strategy

Determination of Manipulation Strategy (module (A) in Fig.1) selects the strategy for manipulation. In this paper determining a manipulation strategy is defined as deciding the following precondition:

- which end-effector or contact points on the robot are to be used
- which contact points on the object are to be made contact with
- what object trajectory is to be referred

For example, if the system selects a single-armed manipulation strategy, the robot makes contact with the object using by the end-effector of the selected arm. Then, the object trajectory and the grasping point on the object, which are both given in advance for single-armed manipulation, are selected. Although in this paper the object trajectory and information about the grasping points for each manipulation strategy are described by programmers, it is preferable that they are automatically generated from the shape and the mass properties of the object or learned from teaching by a human. In this paper we prepare the following strategies:

(a) the single-armed manipulation strategy
(b) the dual-armed manipulation strategy
(c) the full-body contact manipulation strategy

Please note that the above mentioned list of strategies does not describe the optimal and strict classification of how to manipulate the object. For example, (c) includes different manipulation forms in which the robot utilizes the whole arms, the chest and the legs.

Our system selects an adequate manipulation strategy from the above mentioned strategy candidates by evaluating each manipulation by deciding, for example, whether the manipulation is dynamically executable, whether the object trajectory and the information about the grasping points for the object are adequately prepared, and so on. Manipulation strategy selection will be explained in detail in V. If the system cannot find an adequate manipulation strategy, the system should try graspless manipulation.

B. Estimation of the Operational Force based on the Measurement of the Difference between Feedback Forces

In this subsection we present a method to estimate the operational force applicable to an object with an unknown

weight. Measurement of the adequate force for manipulation is significant especially in case of an object with an unknown weight. Some observer may be applied to manipulation of an object with an unknown weight [10]. The feature point of our method is that it is explicitly measured whether the object is moved or not.

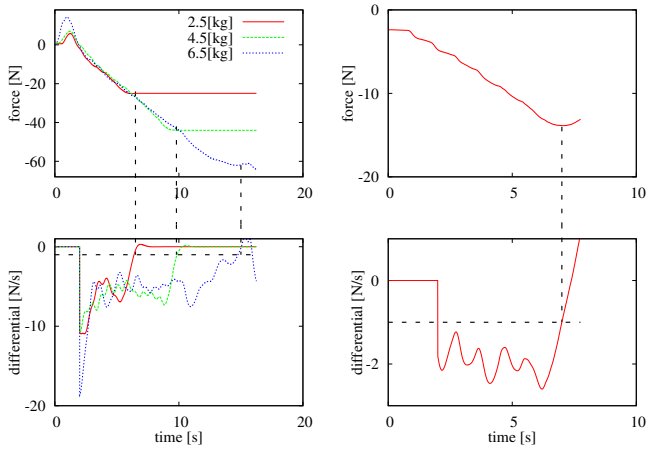

Fig. 2. Result of Picking-up Motion Fig. 3. Result of Pushing Motion
Top graphs : Sum of the measured force at the hands
Bottom graphs : Force Differential
Horizontal dotted lines : Threshold ($\pm 1[N/s]$)
These graphs show that defining a force differential threshold is useful for detecting the time when the object starts to move (vertical dotted lines).
In this case we do not calculate the differential from 0[s] to 2[s]. Since, in the initial 2[s], the robot starts to make contact with the object, and since contact between the robot and the object may be unstable, we neglect the calculation of the differential during the initial 2[s].

1) Estimation based on the Difference between Feedback Forces: This section describes a new method to estimate the operational force focusing on difference between the reaction forces. The estimation method is based on the following assumption: (a) The robot increases the force applied on the object from the start of contact with it quasi-statically. (b) The condition of the contact between the robot and the object does not change during estimation. For example, the robot does not lose its grasp on the object during estimation. Under this assumption, when the object starts to move the reaction force acting on the robot does not exceed a certain value for following reasons: In the case that the operational force is applied against the friction force (for example, in pushing motion), when the object starts to move the robot is affected by a smaller force than the maximum static friction. In the case that the operational force is applied against the gravity force (for example, in picking-up motion), when the object starts to move the robot is affected by a smaller force than the gravity. Our system also detects the change of the condition of the contact between the robot and the object by measuring the reaction force. When the rapid decrease of the reaction force is detected while the robot tries to increase the force applied on the object, the system detects the change of the condition of the contact. For example, the time when the robot loses its grasp on the object during estimation is defined as the failure of estimation.

Therefore we employ the difference between forces to detect the timing of the object's movement. The estimation procedure is as follows: The robot

1) starts to make contact with the object
2) increases force quasi-statically
3) measures the time when the object starts to move using threshold processing of the force differential
4) determines the reaction force at that time to be the estimated operational force

2) Experimental Results of Estimation: Fig.2 and Fig.3 show the measured data of the reaction force. Fig.2 corresponds to a picking-up motion in which the weight of the object are 2.5, 4.5, 6.5[kg] (a basket with plastic bottles) and Fig.3 to a pushing motion. The top graphs show the reaction force at the hands and the bottom graphs are the force differential.

In each graph the robot started estimation at time $= 0[s]$. The plotted data becoming horizontal indicates that the object was moved by the operational force. The timing can be determined by threshold of the force differential. These graphs show that our estimation method can detect the object motion and estimate the operational force.

IV. FORCE BALANCE CONTROLLER FOR FORCE CONTROL AND FULL-BODY BALANCE MAINTENANCE

In this section we present the real-time controller for controlling the reaction force and maintaining full-body balancing (here we call it "Force Balance Controller"). Our control method is suitable to a position-controlled robot. Fig.4 shows the detailed block diagram of the Force Balance Controller, which consists of the following two modules:

- Impedance Controller for Force Control
  The Impedance Controller controls indirectly the reaction force or torque by converting the difference between the commanded force or torque and the measured force or torque into the difference of the position.
- Auto Balancer[11] for Full-Body Balancing
  The Auto Balancer is based on two steps: (a) calculating the COG (Center Of Gravity) trajectory adaptive to the external force (the green dotted square in Fig.4), and (b) calculating the posture sequence according to the kinematic constraint and the COG constraint (the red dotted square in Fig.4).

To calculate the posture sequence $\boldsymbol{\theta}$ as a controller output, this controller requires three kinds of inputs : the kinematics and COG constraint from the Full-Body Motion Generator (module (C) in Fig.1), the operational force constraint based on the Estimaiton of the Operational Force (module (B) in Fig.1) and the feedback sensor data from the real robot (these are respectively shown in Fig.4 as the blue dotted square, the yellow dotted square and the purple dotted square). The variables subscripted with l represent the parameters for the limb controlled by the end-effector and

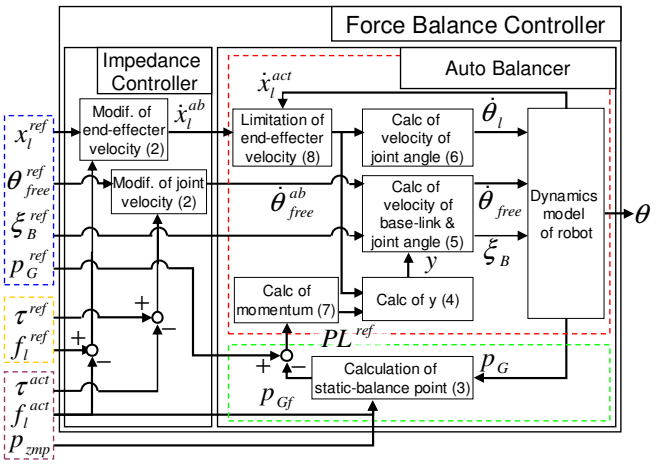

Fig. 4. Configuration of Force Balance Control
Red dotted square : Calculation of the posture sequence
Green dotted square : Calculation of the COG trajectory
Blue dotted square : Input from module (C)
Yellow dotted square : Input from module (B)
Purple dotted square : Input from the real robot

the variables subscripted with $free$ represent the parameters for the limb not controlled by the end-effector. Here we call former limb a end-effector-controlled limb and latter limb a free limb.

Force Balance Controller is characterized by switching its control mode from the end-effector control mode to the joint control mode. Note that Modif. of end-effector velocity and Modif. of joint velocity in Fig.4 are computed at the same time.

- The end-effector control mode
  When the manipulation strategy is selected from the single-armed manipulation strategy and the dual-armed manipulation strategy, Force Balance Controller switch to this mode. During this mode is choosen, Force Balance Controller controls the force at the end-effectors of the arms modifing the positions of the end-effectors (shown as Modif. of end-effector velocity in Fig.4). In case of HRP2-JSK torso and head are considered as free limbs and arms and legs are as end-effector-controlled limbs.
- The joint angle control mode
  When the manipulation strategy is selected from the full-body contact manipulation strategy, Force Balance Controller switch to this mode. During this mode is choosen, Force Balance Controller controls the torque at each joints of the arms modifing the joint angles (shown as Modif. of joint velocity in Fig.4). In case of HRP2-JSK torso, head and arms are considered as free limbs and legs are as end-effector-controlled limbs.

Compatibility of force control and full-body balancing has been discussed as a difficult problem in related works. Several works based on the passivity realize the full-body balancing without measurement of the contact point or the contact force, have been recently reported[7]. These method premise the torque-controlled system and have yet to be applied to rapid motion such as walking. The method proposed by Evard et al. [8] has been developed for a position-controlled system resembling our work. In comparison to [8], one of the features our method is that our control method requires low computation cost since the Force Balance Controller adopts Resolved Momentum Control[12], proposed by Kajita et al., for the calculation of posture sequence. Therefore, we can afford to implement not only the Force Balance Controller, but also other control modules. For example, in 5[ms] our real-time controller performs self-collision observation[13] and checking for joint overload using a warning beep sound, which are quite important functions in heavy load tasks using the whole body. Another feature is that because of switch between two modes our high frequency controller is applicable to full-body manipulation in which the robot contacts with the object by the contact points more than the end-effectors of the arms.

A. Impedance Controller for Force Control

We apply the impedance control at each arm, which indirectly controls the reactive force. That is to say, this impedance control does not compute torques from the reactive force but compute the difference of the position of the end-effector from the difference of the force.

In case of the end-effector control mode impedance formulation at one arm is described as follows:

$$M\ddot{\boldsymbol{x}}_l + D(\dot{\boldsymbol{x}}_l - \dot{\boldsymbol{x}}_l^{ref}) + K(\boldsymbol{x}_l - \boldsymbol{x}_l^{ref}) = \delta \boldsymbol{f}_l \qquad (1)$$

Let M, D and K be virtual inertia, virtual viscosity and virtual stiffness. Let $\boldsymbol{x}_l$ be the position and orientation vector of the end-effector. Here $\delta \boldsymbol{f}_l = (\boldsymbol{f}_l^{act} - \boldsymbol{f}_l^{ref})$, in which $\boldsymbol{f}_l^{act}$ and $\boldsymbol{f}_l^{ref}$ donate the actual 6-dimension vector of force and moment and the reference vector. dt is the cycle time of this controller. The command position of the end-effector for the Auto Balancer module $\boldsymbol{x}_l^{ab}$ is determined as (2).

$$\begin{aligned} \boldsymbol{x}_l^{ab}(t) &= \frac{M[2\boldsymbol{x}_l^{ab}(t-dt) - \boldsymbol{x}_l^{ab}(t-2dt)]}{M + Ddt + Kdt^2} \\ &+ \frac{Ddt\boldsymbol{x}_l^{ab}(t-dt) + [K\boldsymbol{x}_l^{ab}(t) + \delta \boldsymbol{f}_l]dt^2}{M + Ddt + Kdt^2} \end{aligned} \qquad (2)$$

In case of the joint control mode the command joint angle for the Auto Balancer module $\boldsymbol{\theta}_{free}^{ab}$ is obtained by solving (2) in which $\boldsymbol{x}_l$ is replaced by $\boldsymbol{\theta}_{free}$ and $\boldsymbol{f}_l$ by $\boldsymbol{\tau}_{free}$. These transformer is significant for the position controlled robot.

B. Auto Balancer for Full-Body Balance Maintenance

The Auto Balancer requires inputs such as the command velocities of the end-effector and the joint angles, the command COG trajectory, and the external force feedback from the real robot. The calculation method of our Auto Balancer is based on Resolved Momentum Control[12].

1) Modification of the COG Trajectory: The Force Balance Controller modifies the command COG trajectory according to the external forces. We apply the static balance point [2], [14] to control the COG adaptive to the external forces.

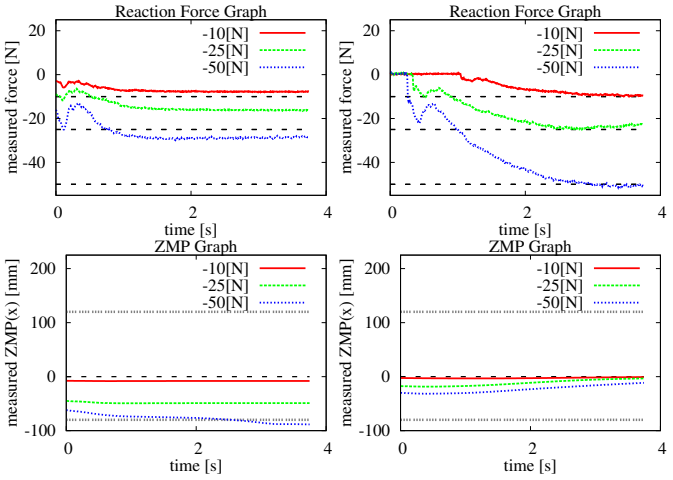

Fig. 5. Reaction Force (Top Graphs) and ZMP (Bottom Graphs)
Top graphs : Dotted lines are reference forces
Bottom graphs : Black dotted line is reference ZMP
Gray dotted lines are edges of the foot polygon
Left graphs : Using only the Impedance Controller.
The robot falls down and following of the force deteriorates.
Right graphs : Using the Impedance Controller and the Auto Balancer.
The robot avoids falling down and the desired force is achieved.

We introduce (3) as x; y components of the static balance point p_{Gfx}; p_{Gfy}. (3) is derived from the equation to calculate the Zero Moment Point (ZMP)[2]. Note that we can adapt (3) to in the case that the object comes in contact with the robot at a contact point that has no force sensor.

$$p_{Gf[x,y]} = \frac{p_{zmp[x,y]}[M(\ddot{p}_{Gz}+g) - \sum_{l\in hand} f_{lz}^{act}]}{Mg - \sum_{l\in hand} f_{lz}^{act}} + \frac{\dot{L}_{G[y,x]} - Mp_{G[x,y]}\ddot{p}_{Gz} + M(p_{Gz} - p_{zmpz})\ddot{p}_{G[x,y]}}{Mg - \sum_{l\in hand} f_{lz}^{act}} \tag{3}$$

Let $[p_{Gx}\ p_{Gy}\ p_{Gz}]^T$ be the COG of the robot and let $[L_{Gx}\ L_{Gy}\ L_{Gz}]^T$ be the angular momentum around the COG. $[p_{zmpx}\ p_{zmpy}\ p_{zmpz}]^T$ denotes the measured ZMP and $[f_{lx}^{act}\ f_{ly}^{act}\ f_{lz}^{act}]^T$ denotes the external force measured at the force sensor except that at the sole. g is the gravity acceleration, and M is the whole mass of the robot.

2) Calculation of the Posture Sequence: The Auto Balancer also calculates the full-body posture sequence based on the command velocities of the end-effectors and the joint angles modified by the Impedance Controller and the command COG trajectory based on the external force.

The Auto Balancer maintains the full-body balancing by controlling the COG position and by keeping the angular momentum low. Since our balancing control module includes the COG position control and angular velocity control, in this paper we call this the Auto Balancer, derived from the original Auto Balancer of our laboratory proposed by Tamiya et al.[11].

In our work, the original Resolved Momentum Control [12] is extended to apply to the Auto Balancer as follows: avoidance of collision and joint angle limits, and the reduction of momentum divergence. First, we employ a method to avoid joint limits based on a weighted least-norm solution[15]. Using this method the weight of the joint which to get acquainted with the limit becomes small. Second, we employ a method to avoid the self-collision by utilizing the redundancy of an arm [16], [17]. Considering these extension we obtain the following equation to calculate the joint velocities. We obtain $\dot{\boldsymbol{\theta}}_{free}$ and $\boldsymbol{\xi_B}$ from (4) and (5) and $\dot{\boldsymbol{\theta}}_l$ from (6).

$$\boldsymbol{y} = \boldsymbol{S}\left\{ \begin{bmatrix} \boldsymbol{P}^{ref} \\ \boldsymbol{L}^{ref} \end{bmatrix} - \sum_{l\in limbs} \begin{bmatrix} \boldsymbol{M}_l \\ \boldsymbol{H}_l \end{bmatrix} \boldsymbol{J}_l^{\dagger} \dot{\boldsymbol{x}}_l^{ab} - \sum_{l\in limbs} \begin{bmatrix} \boldsymbol{M}_l \\ \boldsymbol{H}_l \end{bmatrix} (\boldsymbol{E} - \boldsymbol{J}_l^{\dagger}\boldsymbol{J}_l)\boldsymbol{n}_l \right\} \tag{4}$$

$$\begin{bmatrix} \dot{\boldsymbol{\theta}}_{free} \\ \boldsymbol{\xi}_B \end{bmatrix} = \boldsymbol{A}^{\dagger}\boldsymbol{y} + (\boldsymbol{E} - \boldsymbol{A}^{\dagger}\boldsymbol{A}) \begin{bmatrix} \dot{\boldsymbol{\theta}}_{free}^{ab} \\ \boldsymbol{\xi}_B^{ref} \end{bmatrix} \tag{5}$$

$$\dot{\boldsymbol{\theta}}_l = \boldsymbol{J}_l^{\dagger}\left(\dot{\boldsymbol{x}}_l^{ab} - \begin{bmatrix} \boldsymbol{E} & -\hat{\boldsymbol{r}}_{B\to l} \\ \boldsymbol{0} & \boldsymbol{E} \end{bmatrix} \boldsymbol{\xi}_B \right) + \left(\boldsymbol{E} - \boldsymbol{J}_l^{\dagger}\boldsymbol{J}_l\right)\boldsymbol{n}_l \tag{6}$$

We also use the SR-inverse[18] (represented by † in this paper) instead of the pseudo-inverse to avoid the singularity of the manipulator. $\boldsymbol{J}_l$ is a Jacobian matrix calculated from each limb's configuration and $\boldsymbol{E}$ is an identity matrix. Let $\boldsymbol{n}_l$ be null space velocities for self-collision avoidance and $\boldsymbol{n}_l$ is required in (5) and (6). $\hat{\boldsymbol{r}}_{B\to l}$ is a skew symmetric matrix derived from the difference from the base link to the end-effector. $\boldsymbol{M}_l$ and $\boldsymbol{H}_l$ are inertia matrix and $\boldsymbol{A}$ is computed from selection matrix $\boldsymbol{S}$ and inertia matrices based on the momentum equation (see [12]). $limbs$ is a set of end-effector-controlled limbs. l is a limb included in $limbs$.

According to the mode of Force Balance Controller the configuration of (4) - (6) needs to modify. $limbs$ differs by control mode. In addition in case of the end-effector control mode because $\boldsymbol{\theta}_{free}^{ab}$ is not computed from Impedance Controller $\boldsymbol{\theta}_{free}^{ab}$ is substituted by $\boldsymbol{\theta}_{free}^{ref}$.

$\boldsymbol{P}^{ref}$ and $\boldsymbol{L}^{ref}$ denote the command momentum and the command angular momentum respectively. $\boldsymbol{P}^{ref}$ is obtained by solving (7).

$$\begin{aligned} P_x^{ref} &= MK_{px}(p_{Gx}^{ref} - p_{Gf,x}) \\ P_y^{ref} &= MK_{py}(p_{Gy}^{ref} - p_{Gf,y}) \\ P_z^{ref} &= MK_{pz}(z_B^{ref} - z_B) \end{aligned} \tag{7}$$

z_B^{ref} and z_B are the height of the base link. z_B^{ref} is commanded by module (C) in Fig.1 and z_B is the actual base height of the dynamics model used in the Auto Balancer.

Here we explain reduction of momentum divergence. $\dot{\boldsymbol{x}}_l^{ab}$ is input into (4) and (6). When the manipulator suffers from a singularity or a limit, the difference between $\dot{\boldsymbol{x}}_l^{ab}$ and $\dot{\boldsymbol{x}}_l^{act}$, which is the actual velocity calculated from the solved joint velocities, becomes large. In this case compensation of the momentum derived from motion of the manipulator (the second term in (4)) does not work well, and finally

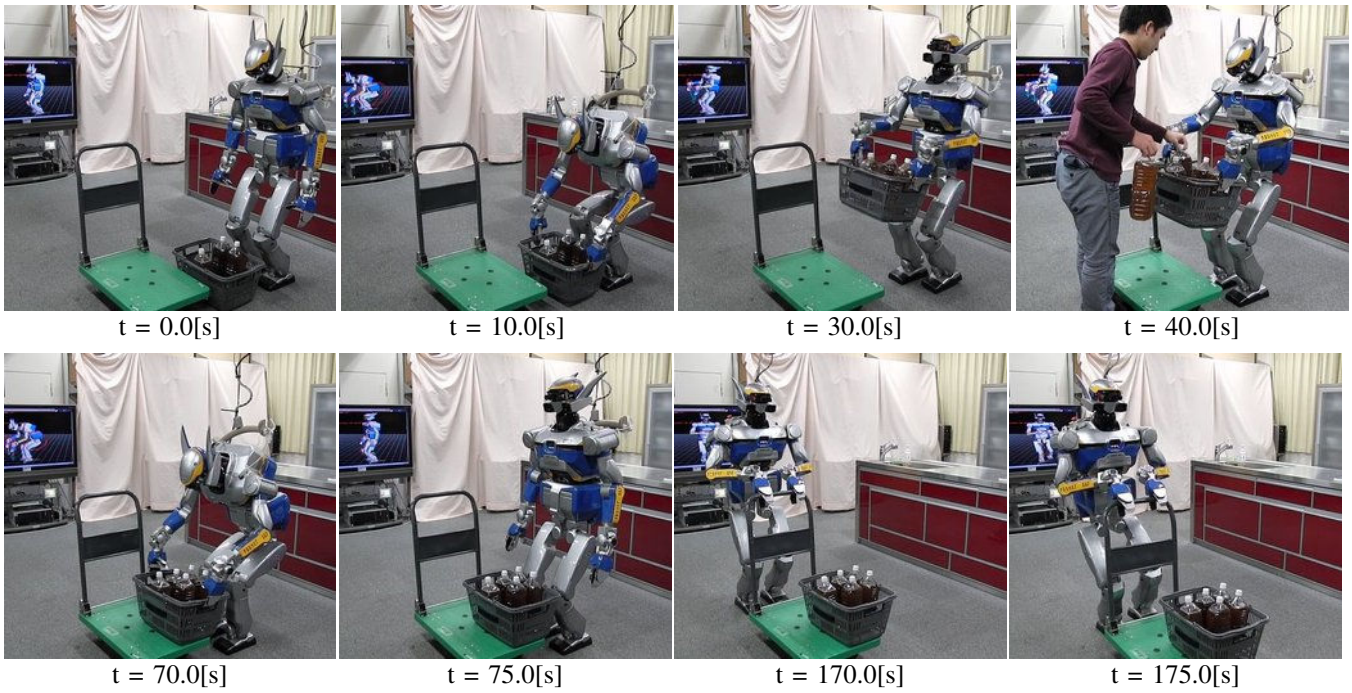

Fig. 6. Experiment of Manipulating an Object with an Unknown Weight
The robot estimated the operational force three times: t = 10[s], t = 40[s] and t = 170[s].
Full-ody control with estimation of the operational force enabled the robot to manipulate the object whose weight changed from 6[kg] to 10[kg].

(4) diverges because we should calculate compensation not based on $\dot{\boldsymbol{x}}_l^{ref}$ but $\dot{\boldsymbol{x}}_l^{act}$. The Auto Balancer eases this divergence by limiting $\dot{\boldsymbol{x}}_l^{ab}(t)$ as (8).

$$\dot{\boldsymbol{x}}_l^{ab}(t) \leftarrow \dot{\boldsymbol{x}}_l^{ab}(t) - K_c \boldsymbol{\delta x}_l(t) \tag{8}$$

Let $\boldsymbol{\delta x}_l(t)$ be the difference at the current control step.

$$\boldsymbol{\delta x}_l(t) = \dot{\boldsymbol{x}}_l^{ab}(t - dt) - \dot{\boldsymbol{x}}_l^{act}(t) \tag{9}$$

K_c is the adequate positive coefficient.

C. Experimental Results of Force Balance Controller

In this subsection we provide experimental data of the Force Balance Controller. In this experiment the robot has contact with the object fixed to the environment at the hand's end-effector. The command forces at the end-effector amount to -10[N], -25[N] and -50[N]. The top graphs of Fig. 5 depict the force and the bottom graphs the ZMP.

A humanoid robot cannot be considered as being fixed to the environment. When using the Impedance Controller when a large force is applied, the humanoid robot falls down (see the top left graph of Fig. 5). Using the Force Balance Controller, the Auto Balancer prevents the humanoid robot from falling down (see the bottom right graph of Fig. 5), and the Impedance Controller regulates the reaction force (see the top right graph of Fig. 5).

V. EXPERIMENT

In this section we present two experiments in which the humanoid robot manipulates objects. V-A shows the experiment in which the operational force varies. V-B shows the experiment in which our control system selects the adequate manipulation strategy based on the mass properties of the object.

A. Manipulation Experiment 1

In the experiment shown in Fig.6 the robot performed the following tasks:

1) Picking up a basket with 6-[kg] plastic bottles(t=10[s])
2) Moving to a cart holding the basket(t=30[s])
3) Holding the 10-[kg] basket while weight was added by a human (t=40[s])
4) Putting down the basket onto a cart (t=70[s])
5) Moving to the handle of the cart (t=170[s])
6) Pushing the cart with the basket loaded onto it (t=175[s])

Before manipulation the control system considered the weight of the object as 0[kg] because the precise weight was unknown.

In this experiment the control system estimated the operational force three times at 1), 3) and 6). Since at 1) and 6) the robot started estimating on the condition that the object was in contact with the environment, the estimation method proposed in III-B.1 was executed. In 1) the estimated operational force for the 6-[kg] weight was 58.924[N] and at 6) for the pushing was 14.973[N] (this is the sum of the forces at both arms). This experiment showed that the presented control system including estimation of the operational force enables the robot to manipulate the object in the case that the weight 1) or the friction coefficient 6) is unknown. Since in 3) the object is in contact with only the robot the mass and the centroid can be estimated using the force sensors at the hands.

Fig. 7. Experiment of Selecting an Appropriate Manipulation Strategy
Although the robot tried to lift the 12[kg] box using both arms, it gave up manipulation because of overloading of the joints at t = 15.0[s]. After switching to the full-body manipulation, the robot was able to lift the box at t = 50.0, 57.0, 75.0[s].

During this experiment the system selected the dual-armed manipulation strategy because the basket model and the cart model have the grasping points for the dual-armed manipulation. The control mode of Force Balance Controller was the end-effector control mode in this case.

Estimation of the operational force is necessary for the cases in which the content of the object changes, for example, as in the case in which a human adds plastic bottles, or a plastic bottle drops out of the basket. Note that measurement of the reaction force is insufficient for estimation of the state of the object. For example, when an increase of the reaction force is detected, it is impossible to determine whether the robot has to struggle to stay on its feet because of an increase in the mass of the content or adapt to the environment. Although we will not discuss this problem in this paper, observation of the state of the object using visual information may be a significant solution. In this experiment the robot started estimating when the trigger based on human detection was observed.

B. Manipulation Experiment 2

Fig.7 shows an example of manipulation strategy switching. Manipulation strategy switching occurred twice in this experiment.

1) Single-Armed Strategy to Dual-Armed Strategy
First, the single-armed strategy was selected and the system tried to solve Full-Body Inverse Kinematics using the end-effector of the selected arm according to the object trajectory for single-armed manipulation. However, the system had no description of the grasping point for single-armed manipulation because of the size of the object. The system discarded the single-armed strategy and adopted the dual-armed manipulation strategy. The end-effector control mode was selected as the control mode of the Force Balance Controller.
2) Dual-Armed Strategy to Full-Body Contact Strategy: Full-Body Motion Generator (module (C) in Fig.1) successfully computed the full-body posture sequence according to the grasping point trajectory for the end-effectors of each arm, and the posture sequence was executed on the real robot. During manipulation, the system evaluated whether manipulation is possible or not. In our setup we employ a function that monitors joint overloading. In the beginning of the dual-armed manipulation, the robot estimated the force for manipulation (see t=15[s] in Fig.7). While the robot was estimating the overload of the wrist-pitch joint of the left arm exceeded the threshold, and the system determined that the dual-armed manipulation strategy was unable to be executed (see the left graph of Fig.9 and the left picture of Fig.8). After module (A) in Fig.1 switched manipulation strategies to full-body contact manipulation and module (D) in Fig.1 selected the joint control mode, the robot resumed manipulation. During manipulation the robot completed the task because of the low overload (see the right graph of Fig.9 and the right picture of Fig.8). This shows that the proposed manipulation strategy switching is useful in the manipulation of heavy loads.

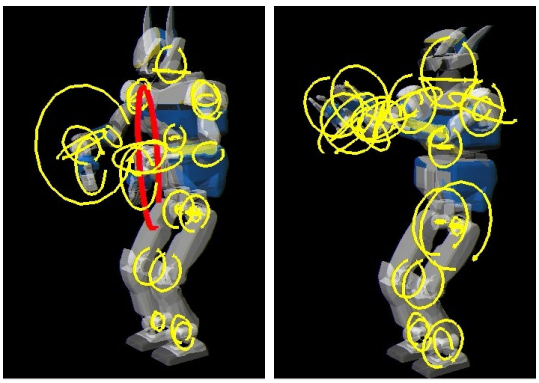

Fig. 8. The Robot Model with Torques Display
Colored circles : Joint torque of each joint.
The radius corresponds to torque ratio and the direction to the frame of the joint.
Yellow circles : Under the threshold (60%)
Red circles : Over the threshold (60%)
Left : In dual-armed strategy at t = 15.0[s], the torque at the wrist-yaw joint of left arm exceeds the threshold.
Right : In fullbody strategy at t = 75.0[s], load distribution is achieved.

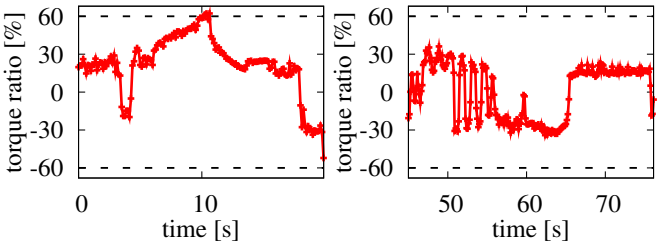

Fig. 9. Torque Ratio (Wrist-Yaw Joint of Left Arm)
Dotted lines : threshold ($\pm 60\%$)
Left : In dual-armed strategy, torques exceeds the threshold
Right : In fullbody strategy, torques is subthreshold

VI. CONCLUSIONS AND FUTURE WORKS

In this paper we introduced a new control system the manipulation of a heavy object for a humanoid robot.

We presented a method to determine the manipulation strategy based on on-line estimation of the operational force. We also presented a high-frequency controller that both controls the external force and maintains full-body balance.

The feature point of our work is that since a full-body control system includes the ability to switch manipulation strategies based on the operational force estimated on-line, the system enables a humanoid robot to manipulate heavy objects as well as light objects. The usefulness of our method was shown in two manipulation experiment examples.

We tested the manipulation tasks of carrying 6- to 12-[kg] loads. Our future work will consist of the challenge of manipulating of heavier objects. Using the proposed method we can try manipulation of a larger load, since we executed the manipulation on the safe side (torque ratio $< 60\%$) in our experiment. We will test the manipulation of heavier objects safely using the high-powered humanoid robot produced in our laboratory[19].

REFERENCES

[1] M.Onishi, Z.W.Luo, T.Odashima, S.Hirano, K.Tahara, and T.Mukai. Generation of Human Care Behaviors by Human-Interactive Robot "RI-MAN". In *Proceedings of The 2007 IEEE International Conference on Robotics and Automation*, pp. 126–127, April, 2007.

[2] Kensuke Harada, Shuuji Kajita, Hajime Saito, Mitsuharu Morisawa, Fumio Kanehiro, Kiyoshi Fujiwara, Kenji Kaneko, and Hirohisa Hirukawa. A Humanoid Robot Carrying a Heavy Object. In *Proceedings of The 2005 IEEE International Conference on Robotics and Automation*, pp. 1724 – 1729, April, 2005.

[3] Y. Ohmura and Y. Kuniyoshi. Humanoid robot which can lift a 30kg box by whole body contact and tactile feedback. In *In Proceedings of the 2007 IEEE/RSJ International Conference on Intelligent Robots and Systems (IROS'07)*, pp. 1136–1141, October, 2007.

[4] Hitoshi Arisumi, Sylvain Miossec, Jean-Remy Chardonnet, and Kazuhito Yokoi. Dynamic Lifting by Whole Body Motion of Humanoid Robots. In *In Proceedings of the 2008 IEEE/RSJ International Conference on Intelligent Robots and Systems (IROS'08)*, pp. 668–675, September, 2008.

[5] Kei Okada, Mitsuharu Kojima, Satoru Tokutsu, Yuto Mori, Toshiaki Maki, and Masayuki Inaba. Task guided attention control and visual verification in tea serving by the daily assistive humanoid hrp2jsk. In *In Proceedings of the 2008 IEEE/RSJ International Conference on Intelligent Robots and Systems (IROS'08)*, pp. 1551–1557, September, 2008.

[6] Luis Sentis and Oussama Khatib. A Whole-Body Control Framework for Humanoids Operating in Human Environments. In *Proceedings of The 2006 IEEE International Conference on Robotics and Automation*, pp. 2641–2648, May, 2006.

[7] Sang-Ho Hyon, Joshua G. Hale, and Gordon Cheng. Full-body compliant human-humanoid interaction: Balancing in the presence of unknown external forces. *IEEE Transactions on Robotics*, Vol. 23, No. 5, pp. 884–898, 2007.

[8] Paul Evrard, Nicolas Mansard, Olivier Stasse, Abderrahmane Kheddar, Thomas Schaus, Carolina Weber, Angelika Peer, and Martin Buss. Intercontinental, Multimodal, Wide-Range Tele-Cooperation Using a Humanoid Robot. In *In Proceedings of the 2009 IEEE/RSJ International Conference on Intelligent Robots and Systems (IROS'09)*, pp. 5635–5640, October, 2009.

[9] Kei Okada, Takashi Ogura, Atsushi Haneda, Junya Fujimoto, Fabien Gravot, and Masayuki Inaba:. Humanoid Motion Generation System on HRP2-JSK for Daily Life Environment. In *International Conference on Mechatronics and Automation*, pp. 1772 – 1777, July, 2005.

[10] Jaeheung Park and Oussama Khatib. Robust haptic teleoperation of a mobile manipulation platform. In *International Symposium on Experimental robotics*, pp. 543–554, June, 2004.

[11] S. Kagami, F. Kanehiro, Y. Tamiya, M. Inaba, and H. Inoue. AutoBalancer: An Online Dynamic Balance Compensation Scheme for Humanoid Robots. In *Robotics: The Algorithmic Perspective, Workshop on Algorithmic Foundations of Robotics(WAFR)*, pp. 329–340, 2001.

[12] S.Kajita, F.Kanehiro, K.Kaneko, K.Fujiwara, K.Harada, K.Yokoi, and andH.Hirukawa. Resolved Momentum Control:Humanoid Motion Planning based on the Linear and Angular Momentum. In *In Proceedings of the 2003 IEEE/RSJ International Conference on Intelligent Robots and Systems (IROS'03)*, pp. 1644–1650, October, 2003.

[13] Kei Okada and Masayuki Inaba. A hybrid approach to practical self collision detection system of humanoid robot. In *In Proceedings of the 2006 IEEE/RSJ International Conference on Intelligent Robots and Systems (IROS'06)*, pp. 3952–3957, October, 2009.

[14] Kensuke Harada, Shuuji Kajita, Kenji Kaneko, and Hirohisa Hirukawa. Lifting motion of an object by a humanoid robot. In *The 27th Annual Conference of the Robotics Society of Japan*, p. 1L17, September, 2004.

[15] Tan Fung Chan and Rajiv V. Dubey. A weighted least-norm solution based scheme for avoiding joint limits for redundant joint manipulators. In *Robotics and Automation, IEEE Transactions on*, pp. 286–292, April, 1995.

[16] H. Sugiura, M. Gienger, H. Janssen, and C. Goerick. Real-time self collision avoidance for humanoids by means of nullspace criteria and task intervals. In *Proceedings of the 2006 IEEE-RAS International Conference on Humanoid Robots*, pp. 575–580, December, 2006.

[17] Hisashi Sugiura, Michael Gienger, Herbert Janssen, and Christian Goerick. Real-time collision avoidance with whole body motion control for humanoid robots. In *In Proceedings of the 2007 IEEE/RSJ International Conference on Intelligent Robots and Systems (IROS'07)*, pp. 2053 – 2068, October, 2007.

[18] Y.Nakamura and H. Hanafusa. Inverse kinematic solutions with singularity robustness for robot manipulator control. *Journal of Dynamic Systems, Measurement, and Control*, Vol. 108, pp. 163–171, 1986.

[19] Junichi Urata, Toshinori Hirose, Namiki Yuta, Yuto Nakanishi, Ikuo Mizuuchi, and Masayuki Inaba. Thermal control of electrical motors for high-power humanoid robots. In *In Proceedings of the 2008 IEEE/RSJ International Conference on Intelligent Robots and Systems (IROS'08)*, pp. 2047–2052, September, 2008.